Enhanced Meta-Heuristic Approach for Echo Suppression in Synthetic Aperture Radar Using Non-Periodic Interrupted Sampling

Anoosha Chukka[1]*[ID], Tirumala Krishna Battula[2][ID]

[1] Department of ECE, Anil Neerukonda Institute of Technology and Sciences, Visakhapatnam 531162, India
[2] Department of ECE, Jawaharlal Nehru Technological University Kakinada, Kakinada 533003, India

Corresponding Author Email: anushachukka@gmail.com

ABSTRACT

Echo cancellation is a deception jamming technique designed to nullify the target's echo and prevent its detection by enemy radar. Traditional methods rely on time-domain synchronization, but they struggle to fully suppress echoes when there is an amplitude mismatch. This limitation often leaves the target partially visible in synthetic aperture radar (SAR) images, reducing the effectiveness of the jamming technique. Non-periodic interrupted sampling modulation (NP-ISM) is applied as it produces a continuous jamming strip instead of discrete false targets whereas in Periodic sampling multiple false targets emerge even the real target echo is canceled which makes it easy to be countered by enemy radar. The improved henry gas solubility optimization algorithm (IHGSOA) is applied in the echo cancellation model to optimize the random rectangular envelope pulse train in the NP-ISM which enhances signal cancellation. This significantly reduces the Peak to Average Ratio (PAR), enabling more effective target echo suppression. A polynomial non-linear frequency modulation (PNLFM) is employed to reduce the PAR leading to significant improvement in signal-to-noise ratio (SNR), enabling more effective target echo cancellation. The proposed IHGSOA-based echo cancellation model effectively aligns the cancellation and echo signals through time-delay synchronization, minimizing errors even in the presence of a mismatch. The simulation results show that using the above cancelling system the desired target echo amplitude drops to 50% and 40% of its original target echo, hence the system has a very high cancellation effect. Thus, the effectiveness of the IHGSOA is evaluated by comparing its performance with other conventional algorithms.

1. INTRODUCTION

Due to the increase in imaging technologies, the SAR plays an essential role in both military aspects and civil. SAR jamming includes a variety of techniques that have been developed in order to prevent the tracking of Target of Echo (TOI) by the SAR [1]. Blanket jamming and deception jamming are examples of SAR jamming techniques. Further, SAR jamming is often divided into two categories such as barrage jamming and misleading jamming [2]. The processed SAR image has been greatly impacted by barrage jamming, especially in the TOI region. A distorted image of the TOI is formed with the aid of deceptive jamming, making it difficult to figure out the TOI [3].

According to theory of echo cancellation, by finding the cancellation echo—a synthetic replica of the echo signal itself unwanted echoes may be eliminated. Suppressing the target echo at the radar receiver using echo cancellation is a good technique that protects the TOI [4]. The basic premise of echo cancellation is the generation of echo cancellation signal i.e., the copy of the target echo by an active source to the radar so that both target echo and cancellation echo reach the radar. Numerous studies regarding the use of echo cancellation have been conducted during the last few decades [5]. Over a

significant number of studies, it has been taken into account as essential for synchronization in the amplitude and time is required [6]. From the previous research works on echo cancellation, The SAR has the ability to pass signals with a wide temporal bandwidth, such as LFM pulses. Thus, at the SAR receiver, a canceled signal may arrive after the target echo. As they used amplitude and time-delay modulation in the cancellation technique [7]. Since there is an amplitude mismatch, the target echo is able to be totally deleted from the SAR images and stays apparent in the SAR image [8].

In order to mitigate the issues in the SAR, a canceled echo can actually stay behind the target one [9]. This happens when SAR receives and transmits large "Time Bandwidth Product (TBP)" signals like LFM pulses, and the production phases of echo cancellation need adequate processing time. Since delayed echo signal and original echo have distinct frequencies, and this situation will lead to cancellation failure [10]. ISRJ is commonly employed to disable radar fake behavior, and it includes Inverse SAR (ISAR) and SAR [11]. Most recently, the ISRJ approach has been employed to perform delayed cancellation echo; nevertheless, this technique fails quickly since several fake targets arise while the true target echo is canceled [12].

In order to maintain good resolution and to get suppressed

side lobes of the signal, one can use an improved Non-Linear Frequency Modulation (NLFM) polynomial signal. To have a low side lobe and high Peak to Average Ratio (PAR) a Polynomial NLFM signal is used [13]. This research presents a novel idea for echo cancellation in SAR using heuristic algorithms.

The most important contributions of the heuristic aided-echo cancellation model are enumerated as follows:

- To flourish the heuristic-assisted echo cancelation model in SAR to cancel the target echo at the receiver of the SAR so the chance of detection of TOI is prevented.
- To augment the performance of the heuristic assisted-echo cancelation model, an IHGSOA is offered. It is employed to optimize the rectangular envelope pulse train in NP-ISM so the PAR value is lowered.
- The results generated by the IHGSOA-based echo cancellation model are examined with the traditional echo cancellation system to determine the overall capability of the recommended echo cancellation model.
- A Polynomial Non-Linear Frequency Modulation (PNLFM) is used to reduce the peak side lobes and to increase the SNR and PAR, so that the target echo is canceled effectively.

The balance parts of the IHGSOA-based echo cancellation model are prearranged as follows. Segment II gives the prior echo cancellation models and their uses and limitations. In segment III, the basic signal model of echo cancellation based on incidence and time-delay modulation and the impacts caused by amplitude mismatch for echo cancellation is elaborately given. The NP-ISM pulse characteristics, modulated Polynomial NLFM signal characteristics and procedure of the developed model are categorized in segment IV. In segment V, conventional HGSOA, implemented IHGSOA, IHGSOA-based optimal NP-ISM is presented in a brief way. In segment VI, the results and conversation of the explored echo cancellation model in SAR are given. The final segment, VII gives the conclusion of the recommended echo cancellation model.

2. LITERATURE AND PROBLEM STATEMENT

Synthetic Aperture Radar (SAR) plays a crucial role in both military and civilian applications due to its high-resolution, all-weather, and long-distance imaging capabilities. To mitigate issues in SAR detection, various jamming techniques have been developed. The non-periodic interrupted sampling repeater jamming (ISRJ) technique [14] provides robust cancellation performance by generating jamming strips to protect the target of interest (TOI), minimizing the need for precise parameters. The three-stage active cancellation method [15] eliminates target echoes without requiring exact time matching but struggles with amplitude mismatches. Counter ISRJ [16] remains effective under certain error conditions but faces high cancellation effects. Non-Linear Frequency Modulation (NLFM) [17] is an easy-to-implement process, though it does not operate in the frequency domain. Improved ISRJ [18] generates false targets for deception jamming, while Ground Moving Target Detection (GMTD) [19] effectively identifies moving targets and suppresses unwanted echoes, proving more effective than other methods for non-stationary targets. These techniques collectively enhance SAR jamming performance, though challenges remain.

Despite advancements in SAR jamming techniques, current methods face limitations in effectively cancelling target echoes under varying conditions. but further enhancement is needed to achieve more effective echo cancellation. Therefore, there is a need for a novel jamming model that can overcome these limitations, offering enhanced echo cancellation and improved SAR jamming performance.

The objective of this research is to develop a novel technique for radar echo cancellation in SAR systems by utilizing NP-ISM combined with an improved Meta-Heuristic optimization algorithm.

3. SIGNAL MODEL OF ECHO CANCELLATION FOR SAR

3.1 Basic signal model of echo cancellation based on frequency and time-delay modulation

The SAR consists of a target and a canceller. The trajectory of the SAR is identified from the dashed line. The Line of Sight (LOS) is placed in between the SAR to the target, and here canceller is placed on this LOS of the SAR geometry. The target is pointed by the receiver antenna, and the SAR is pointed by the transmitter antenna, and both of these antennas are positioned in the canceller. In SAR, the echo cancellation is completed by three steps. The goal echo is intercepted by the canceller in the initial step of this procedure. Afterward, the attributes of the signal are examined to develop the cancellation signal. To this end, the antennas are employed to determine the transmitting power, and this transmitting power is retransmitted to the SAR for the echo cancellation [20].

The LFM signal transferred to the SAR without any loss of simplification is elucidated in Eq. (1):

$$s(t) = v(t) \, exp(j2\pi g_0 t + j\pi l t^2) \qquad (1)$$

where,

$$v(t) = rect \frac{t}{U} \qquad (2)$$

Here, the width of the pulse is indicated as U, the chip rate is illustrated as l, the fast time is signified as t, and the middle of frequency is elucidated as g_0. The Eq. (3) shows expression for the baseband echo.

$$s_e(t, t_n) = v\left(t - \frac{2R(t_n)}{c}\right) exp\left(j2\pi g_0 \frac{2R(t_n)}{c}\right)$$
$$. exp\left\{j\pi l \left(t - \frac{2R(t_n)}{c}\right)^2\right\} \qquad (3)$$

Here, the distance in the middle of the radar and the target is represented as $R(t_n)$, slow time is indicated as t_n, and the propagation speed of the EM is indicated as c [18]. The symbolic form of outcome is indicated in Eq. (4):

$$I_e(t, t_n) = sin \, c\left(\frac{t - \frac{2R_{min}}{c}}{\varpi_r}\right) sin \, c\left(\frac{t_n - t_c}{\varpi_a}\right)$$
$$. exp\left(-j \frac{4\pi g_0 R_{min}}{c}\right) \qquad (4)$$

Here, when the target and the SAR are very close to each

other, then the slow time is represented as t_c, the smallest distance in the middle of the target and the radar is signified as, R_{min} the resolutions of azimuth and the resolutions of the range is indicated as ϖ_a, and ϖ_r respectively.

$$\varpi_r = \frac{1}{C_r} \tag{5}$$

$$\varpi_a = \frac{1}{c_a} \tag{6}$$

Here, the bandwidth of the signal is represented as C_r and the bandwidth of the azimuth is signified as C_a.

In the receiver of the SAR, the target is canceled if the amplitude of the indication to be canceled and the amplitude of the aim echo must be in the same condition, and it is mathematically given in Eq. (7):

$$s_c(t, t_n) = -s_e(t, t_n) \tag{7}$$

Because of the unavoidable time delay τ_d, the signal to be canceled is lag on the target echo, and it is elucidated in Eq. (8):

$$\hat{s}_c(t, t_n) = -s_e(t - \tau_d, t_n) \tag{8}$$

Here, the assumption is $\tau_d \neq 0$. It is not able to synchronize the signal to cancel and the target echo signal at fast time variable. If the synchronization process is not done for the cancelation signal and the target echo at the fast time variable then it causes failures in the echo cancellation process [21, 22].

At time delay τ_d, the intercepted signal is accompanied by the frequency shift for canceling the baseband received signal, and it is illustrated in Eq. (9):

$$
\begin{aligned}
s_s(t, t_n) = v\left(t - \frac{2R(t_n)}{c} - \tau_d\right) \\
. \exp\left(-j2\pi g_0 \frac{2R(t_n)}{c}\right) \\
. \exp\left\{j\pi l\left(t - \frac{2R(t_n)}{c} - \tau_d\right)^2\right\} \\
. \exp\left\{j\pi g_d\left(t - \frac{2R(t_n)}{c} - \tau_d\right)\right\} . \exp(-j2\pi g_0\tau_d)
\end{aligned}
\tag{9}
$$

The results produced in pictorial form are given in Eq. (10).

$$
\begin{aligned}
I_c(t, t_n) = I_e\left(u - \tau_d + \frac{g_d}{l}, t_n\right) \\
\exp\left\{-j\pi\left(\frac{g_d^2}{l} + 2g_0\tau_d\right)\right\}
\end{aligned}
\tag{10}
$$

The time delay τ_d and the frequency shift g_d must be fulfilled if the $I(t, t_n) = 0$. The time delay τ_d and the frequency shift g_d are identified by Eqs. (11) and (12).

$$\tau_d = -\frac{g_0}{l} + \sqrt{\left(\frac{g_0}{l}\right)^2 + \frac{(2i + 1)}{l}} \tag{11}$$

$$g_d = -g_0 + \sqrt{g_0^2 + (2i + 1)l} \tag{12}$$

For particular time domain, the pictorial outcome of the combined signal is synchronized. This process is done in the reverse direction; the integer is represented as i. The geometric view of the SAR is illustrated in Figure 1.
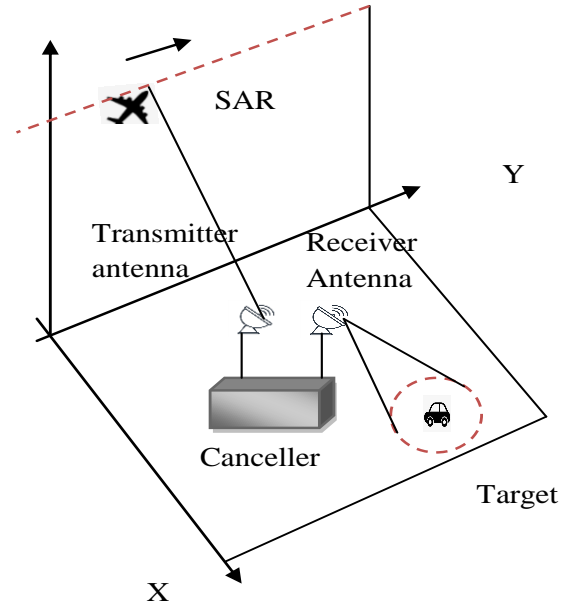

Figure 1. Geometric view of the SAR [2]

3.2 Modulated NLFM and polynomial NLFM signal characteristics

Modulated NLFM and Polynomial NLFM signals are designed to enhance range resolution and suppress sidelobes in radar systems. Polynomial NLFM offers better control over frequency modulation, improving signal-to-noise ratio (SNR) and target detection.

3.2.1 NLFM

Utilizing the NLFM waveform may result in excellent SNR, low noise interference, and high range resolution [23]. When compared to a linear frequency modulated wave, NLFM offers a greater detection range. The NLFM signal is represented as:

$$S(t) = exp[j\emptyset(t)] \tag{13}$$

Here, $\emptyset(t)$ is a frequency modulation function, and f(t) may be obtained via differentiation phase of Eq. (1). No weighting mechanism is needed to reduce side lobes in the NLFM waveform. Improved NLFM refers to an NLFM signal that is intended for varied time sweeps. The bandwidth and overall time sweep are divided into two and three stages, respectively, via improved NLFM. The side lobe level at first peak of -17.62dB is achieved after autocorrelation of the tri-stage NLFM signal, which is lower than the two-stage NLFM. To further lower PSL, an Improved Polynomial-I & II NLFM is devised for different BT values. It can be seen that the lowered PSL for conventional approaches is insufficient for many applications in field of radar and sonar. In addition to Tri-stage NLFM, developed Polynomial-I NLFM and Polynomial-II NLFM signals show a drop in the first side lobe level [24].

3.2.2 Polynomial-I and polynomial-II NLFM

Two types of PNLFM waveforms Polynomial-I and Polynomial-II are considered with Uniform and Non-Uniform PRI [24, 25].

$$Sp(t) = exp[j\emptyset(t)] \tag{14}$$

where, $\emptyset(t) = 2\pi \int f(t)$.

Polynomial-I NLFM:

$$fp1(t) = a_1 t^6 - a_2 t^4 + a_3 t^2 \tag{15}$$

Polynomial-II NLFM:

$$fp2(t) = a_1 t^2 - a_2 \sqrt{1 - a_3 t^2} \tag{16}$$

where, a_1, a_2, a_3 are constants and t are the instantaneous time.

4. DEVELOPED OPTIMIZATION-BASED ECHO CANCELLATION MODEL FOR SAR

It focuses on enhancing jamming effectiveness by optimizing echo cancellation techniques. This model influences advanced optimization algorithms, such as the Improved Henry Gas Solubility Optimization Algorithm (IHGSOA), to fine-tune non-periodic interrupted sampling modulation (NP-ISM) for better cancellation of target echoes. By reducing the PAR and improving the synchronization between the cancellation echo and the target signal, this model ensures more reliable protection of the target of interest (TOI) from SAR detection. The approach addresses the limitations of existing jamming techniques.

4.1 NP-ISM pulse characteristics

The rectangular envelope pulse train is present in the interrupted sampling function, and it is illustrated in Eq. (17).

$$p(t) = rect\left(\frac{t}{\tau}\right) \otimes \sum_{n=-\infty}^{+\infty} \delta(t - nTs) \tag{17}$$

where, τ is the sub-pulse width, Ts is the sub-pulse repetition interval, $\delta(\cdot)$ is the impulse function, n is the pulse number, $\otimes$ represents the convolution operation.

Via Fourier transform, the spectrum of $p(t)$ is given as in Eq. (18):

$$P(f) = \tau f_s \sum_{n=-\infty}^{n=+\infty} sinc(nf_s\tau)\, \delta(f - nf_s) \tag{18}$$

$$f_s = \frac{1}{T_s} \tag{19}$$

The NP-ISM frequency is signified in the above Eq. (19).

The interrupted discrete desire function is summed to get the spectrum of the interrupted sampling impulse pulse. Here, the train of false targets is systematically arranged to form the periodic interrupted sample. This sample is utilized for modulating the Matched Filter (MF) output of the LFM signal [21]. The random rectangular pulse train is used to modulate the Non-Periodic Interrupted sample and it is stimulated in Eq. (20).

$$p_A(t) = \sum_{n=0}^{K-1} a_n rect\left(\frac{t - n\tau}{\tau}\right) \tag{20}$$

where, a_n is the code sequence. Non-periodic interrupted sampling pulse is encoded by {0, 1}. τ is the code width, $K=T\tau$ represents the total code number within one pulse.

4.2 The procedure of the developed model

In the intercepted echo, the unavoidable time delay that occurs in the canceller is neglected, and this is considered as the initial step in the echo cancellation process. The second step here is to add the cancellation signal with the NP-ISM at the longest time field. Here, the random rectangular envelope pulse train is optimized by the explored IHGSO for the purpose of lowering the PAR. The final process in the echo cancellation is to forward the signal to the SAR and diminish the usage of energy during the transmitting process. The intercepted target echo cancellation is analyzed to get the controller. From this controller, the controlling attributes are attained to modulate the signal to be canceled on the SAR.
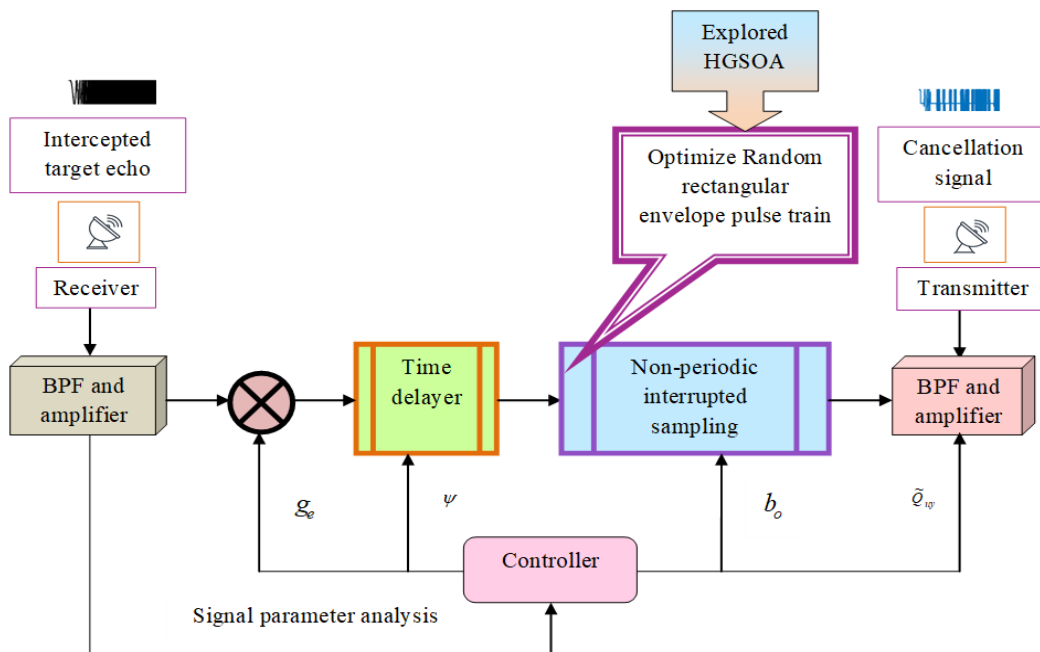

Figure 2. Schematic portrayal of the developed echo cancellation system

The signal to be canceled received on the baseband is formulated in Eq. (21):

$$s(t, t_n) = \varphi_K P_A(t - 2R(t_n)/c)s_s(t,, t_n) \qquad (21)$$

The target echo available in the SAR is avoided by the signal to be canceled. Moreover, the NP-ISM is used to develop the jammed strip, which is also used for neglecting the target echo in the SAR.

The signal to be canceled is not completely ignored if the amplitude mismatch has occurred. Here, the developed model is executed to apply the jamming strip in order to shield the target signal. Additionally, the suggested NP-ISM has the benefit of making radar anti-jamming. If the frequency between the radar-matched filter and the signal to be canceled is very high, then the amplitude of the jamming strip is considerably lowered. Hence, the detection capacity of the radar is lowered by enhancing the energy of the canceller. But missile attack is the major issue associated with the high jamming power. The schematic portrayal of the developed echo cancellation system is signified in Figure 2. ψ represents time delay τ_d, g_e represents sampling frequency g_d, b_0 represents ISRJ 1st coefficient a_0 and $\tilde{Q}_{xy}$ represent transmitting power $P_t(t_n)$ for echo cancellation.

4.3 Dataset description

The echo cancellation in the SAR is done by collecting the data from the ICEYE dataset [26].

Dataset 1 (ICEYE dataset): The SAR images are accumulated from the SAR dataset from the link of "https://www.iceye.com/downloads/datasets" with ingress date: 2023-8-31. This dataset is composed of several products like persistent monitoring, vision, technology and daily change detection. Moreover, the SAR data, imaging models and tasking are available in this dataset.

This dataset is composed of several products like persistent monitoring, vision, technology and daily change detection. It is composed of several SAR images of diverse countries. Moreover, the SAR data, imaging models and tasking are available in this dataset.

5. IHGSOA FOR OPTIMAL NP-ISM IN ECHO CANCELLATION MODEL

The IHGSOA is an advanced meta-heuristic optimization technique inspired by the solubility of gases in liquids. It enhances the original Henry Gas Solubility Optimization (HGSO) algorithm by improving exploration and exploitation capabilities, allowing it to find optimal solutions more efficiently. IHGSO is particularly effective for solving complex, nonlinear problems such as signal processing in radar systems, where it optimizes parameters for tasks like echo cancellation, reducing PAR, and improving overall system performance. Its flexibility and robust search mechanisms make it well-suited for optimizing multi-dimensional and dynamic environments.

Here is a structured outline of the IHGSOA (IHGSO with key steps and mathematical formulations):
1. Initialization
- Population Initialization: Define a population of gas molecules (solutions) X_i for (i = 1, 2,…., N), where N is the population size. Each solution represents a candidate in the search space.

$$X_i = \{x_{i1}, x_{i2}, x_{i3} \ldots . x_{id}\} \qquad (22)$$

where, x_{id} represents the position of the i_{th} solution in the d-dimensional search space.
- Objective Function: Define an objective function $f(X_i)$ to evaluate the quality of each solution.
2. Henry's Law for Gas Solubility
- Henry's Law Constant Calculation: Calculate Henry's law constant H_c for each molecule, which determines the gas solubility and helps balance exploration and exploitation.

$$H_c = H_{min} + (H_{max} - H_{min}) \times rand(0,1) \qquad (23)$$

where, H_{min} and H_{max} are predefined lower and upper bounds of the Henry constant, $rand(0,1)$ is a random value between 0 and 1.
3. Solubility Calculation
- Solubility of Gas Molecules: Calculate the solubility S_i of each molecule based on its current position and Henry's constant.

$$S_i = H_c \times e^{-f(X_i)} \qquad (24)$$

where, $f(X_i)$ is the objective function value for solution X_i, and S_i is the solubility representing the likelihood of exploring that region of the search space.
4. Position Update

Molecule Movement: Update the position of each molecule based on solubility. The new position is influenced by the best solution found so far, X_{best} and random perturbations for exploration.

$$X_i^{new} = X_i^{old} + rand(0,1) \times (X_{best} - X_i^{old}) + \alpha \times rand(-1,1) \qquad (25)$$

where (X_i^{new}) is the updated position, α is a step size control parameter, and $rand(-1,1)$ is a random value between -1 and 1 to introduce randomness.
5. Exploration vs. Exploitation Balance

Adaptive Parameter Tuning: Use dynamic parameter control to balance exploration (searching new regions) and exploitation (intensifying the search around the best solutions). The adjustment of Henry's constant and solubility adapts based on the algorithm's progress.
6. Fitness Evaluation

Update Fitness: Evaluate the new solutions using the objective function X_i^{new}. If the new solution is better than the current best solution, update X_{best}.
7. Convergence Criteria

Stopping Condition: Repeat steps 3 to 6 until the stopping criterion is met (e.g., maximum number of iterations or a sufficiently small change in the best solution).

If $|f(X_{best}) - f(X_{prev})| < \epsilon$ or Maximum iterations reached, stop.
8. Return the Optimal Solution

Final Solution: Once the stopping condition is met, return the best solution X_{best} found by the algorithm.

This framework describes how IHGSO refines gas molecule positions in search space, progressively finding the optimal solution.

The IHGSOA is utilized in the echo cancellation model to

optimize the Random rectangular envelope pulse train in the NP-ISM. So, the value of PAR is greatly lowered so the target echo can be effectively canceled. Moreover, the echo cancellation process is completed within a limited amount of time because of this optimization process. The HGSOA is a physics-inspired algorithm and it can easily defeat complex issues. Additionally, the local optimal issues are easily avoided by the HGSOA. The most important advantage of the HGSOA is it can easily handle the balance in the middle of the examination and the management phase. Yet, it gives only a single solution for the optimization problem. Additionally, it may be stuck in the local optimal condition. To deal with these issues, an IHGSOA is presented. Here, the best and the mean fitness are employed to calculate the new random number and it is specified in Eq. (26):

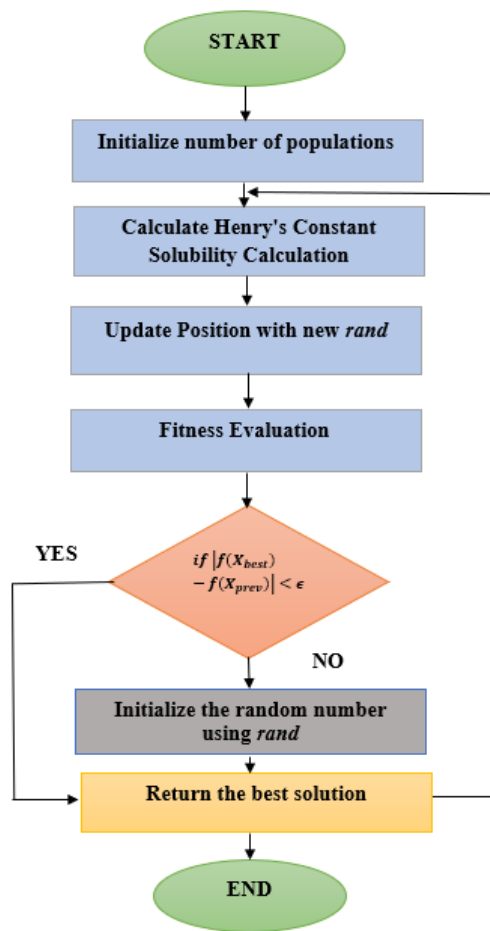$$rand = \frac{X_{best}}{100 * X_{mean}} \qquad (26)$$

Figure 3. Illustration of developed IHGSOA with flow chart

Here, the new random number calculated by the explored IHGSOA is characterized as and the best and the mean fitness is represented as, and respectively. Because of the explored PAR value is greatly lowered. The process flow depiction of the IHGSOA is prescribed in Figure 3.

5.1 IHGSOA-based optimal NP-ISM

The IHGSOA-based optimal non-periodic interrupted sampling intonation process is carried out to cancel the target echo in the SAR. Here, the echo cancellation process is done

in three steps. At first, the inescapable time delay that has occurred on the intercepted echo is avoided. In the second step, at the longest time filed, the cancellation signal is combined with the non-periodic interrupted sampling. Here, the echo present in the signal was canceled via the "NP-ISM" and the random rectangular envelope pulse train in the "NP-ISM" was optimized by the explored IHGSOA. At last, the loss of energy when transferring the signal to the SAR is neglected to achieve an accurate signal. The controller is attained by analyzing the intercepted target signal. Further, the attributes from the controller are used to modulate the termination signal.

The objective function of the IHGSOA-based optimal NP-ISM is used to lower the value of the PAR in the signal, and it is accustomed in Eq. (27):

$$FO = arg \min_{\{rrept\}} (PAR) \qquad (27)$$

Here, the objective function is delineated by the term *FO*, and the random rectangular envelope pulse train is signified as *rrept*, and it lies in the region of [1 to 512], the PAR is estimated by Eq. (28):

$$PAR = \frac{PP}{AP} \qquad (28)$$

Here, the term *PP* gives the peak power, and the term *AP* gives the average power. The solution diagram of the IHGSOA-based optimal NP-ISM is indicated in Figure 4.
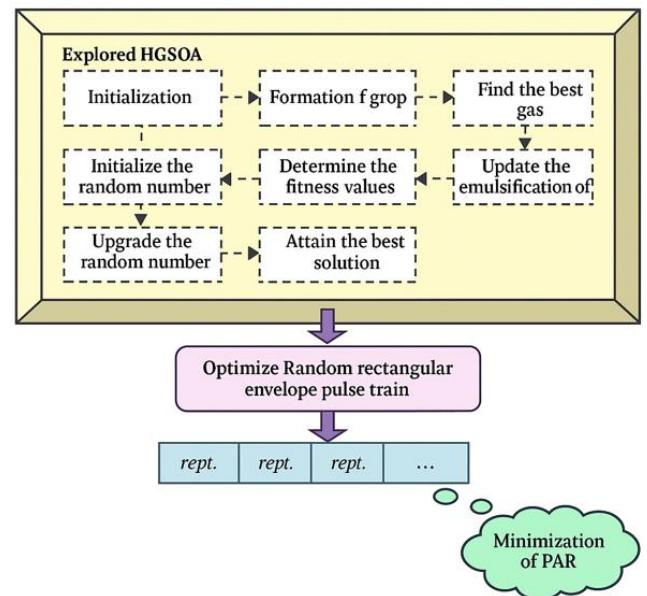

Figure 4. Solution diagram of the IHGSOA-based optimal NP-ISM

The statistical measures used to evaluate the performance of a heuristic-based echo cancellation model are:

i. **Best (Maximum Performance)**

The best performance observed among all the data points of the fitness function. This is the highest value in your dataset. The value represents the optimal performance achieved under the best conditions or settings.

$$Best = \max (X_1, X_2, X_3 \dots \dots , X_n) \qquad (29)$$

ii. **Worst (Minimum Performance)**

The worst performance observed among all the data points

of fitness function. This is the lowest value in your dataset. This value reflects the least favourable performance observed.

$$Worst = \min(X_1, X_2, X_3 \ldots\ldots, X_n) \qquad (30)$$

iii. **Mean**

The sum of all performance values divided by the number of data points of the fitness function. This provides an overall average measure of performance. The mean gives a central value around which the performance data is distributed.

$$Mean = \frac{1}{n}\sum_{i=1}^{n} X_i \qquad (31)$$

iv. **Median**

The middle value when the data points are arranged in ascending order. If there's an even number of data points, it's the average of the two middle values. The median is a measure of central tendency that is less sensitive to extreme values than the mean.

v. **Standard Deviation (SD)**

A measure of the amount of variation or dispersion in the performance data of the fitness function. It shows how much the performance values deviate from the mean. A low standard deviation indicates that the performance values are close to the mean, while a high standard deviation indicates greater variability.

$$SD = \sqrt{\frac{1}{n}\sum_{i=1}^{n}(X_i - Mean)^2} \qquad (32)$$

6. RESULTS AND DISCUSSION

6.1 Simulation setup

MATLAB 2020a platform was adopted to realize the IHGSOA-based echo cancellation method in SAR, and the validation processes were carried out. The experiment was carried out by taking the number of the population as 10 and the utmost iteration as 50. Further, the span of the chromosome was taken by multiplying the mismatch value. Here, the conventional algorithms such as "Gorilla Troops Optimizer (GTO) [27], Salp Swarm Algorithm (SSA) [26], Honey Badger Algorithm (HBA) [28] and HGSO [25]" were taken into consideration to find the efficiency of the urbanized model.

We suppose that the nonperiodic interrupted sampling pulse is with code width τ=2μs, interrupted sampling frequency f_s=1/τ =0.5MHz and pulse width U=100μs. The frequency shift g_d =12.2MHz, time-delay τ_d =0.082μs for the cancellation signal according to Eqs. (11) and (12).

6.2 Cancellation performance of target echo

The productivity images of the IHGSOA-based echo cancellation model are provided in Figure 5.

As shown in Figure 5. when applying the proposed method, the amplitude of cancellation signal matches with target echo at SAR receiver. Therefore, the effective cancellation echo is obtained and which can cancel the target echo. Considered the different SAR images and applied the proposed echo cancellation techniques to cancel the target echo to reach the enemy radar. In Figure 5 of image 1, first figure shows three parts original target signal, the echo signal before cancellation and the echo signal after cancellation. Figure 5(a) shows the original image amplitude without echo cancellation in the first plot, where the amplitude is very high, making the target more visible in the SAR image. With the proposed echo cancellation method, the amplitude is reduced by 50% in Figure 5(a) and by 40% in Figure 5(b), indicating reduced target visibility in the SAR image. Hence, the system has a very high cancellation effect. The system can cancel the target echo effectively.
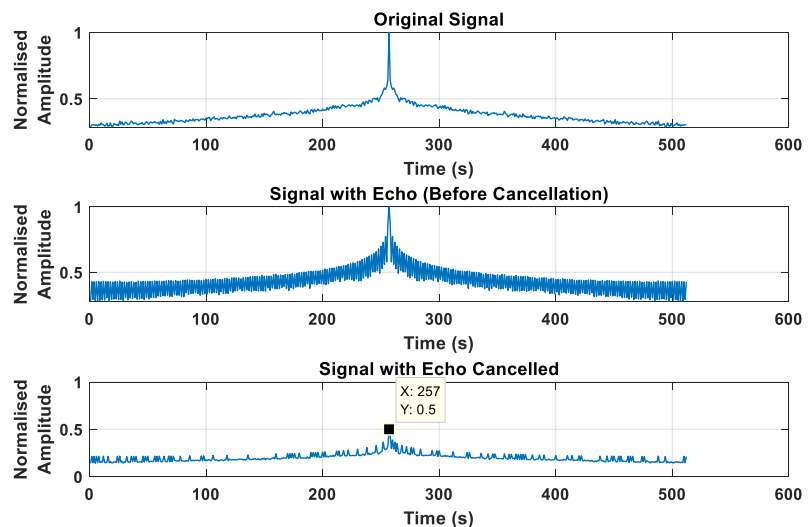
6.3 Convergence assessment

The convergence assessment of the IHGSOA-based echo cancellation method for the SAR is given in Figure 6. From Figure 6(a), the convergence speed of the IHGSOA-based echo cancellation method is better than GTO, SSA, HBA and HGSO with 0.42%, 0.34%, 0.46% and 0.03% at 80th iteration. For the 2nd SAR image, the cost function of the IHGSOA-based echo cancellation model is better than the GTO, SSA, HBA, and HGSO with 0.25%, 0.16%, 0.08% and 0.28% at iteration 100. Similarly, for the 3rd and the 4th SAR images, the value convergence rate is considerably be with an increase in iteration value. Thus, the cost function of the IHGSOA-based echo cancellation method is better than the existing algorithms.
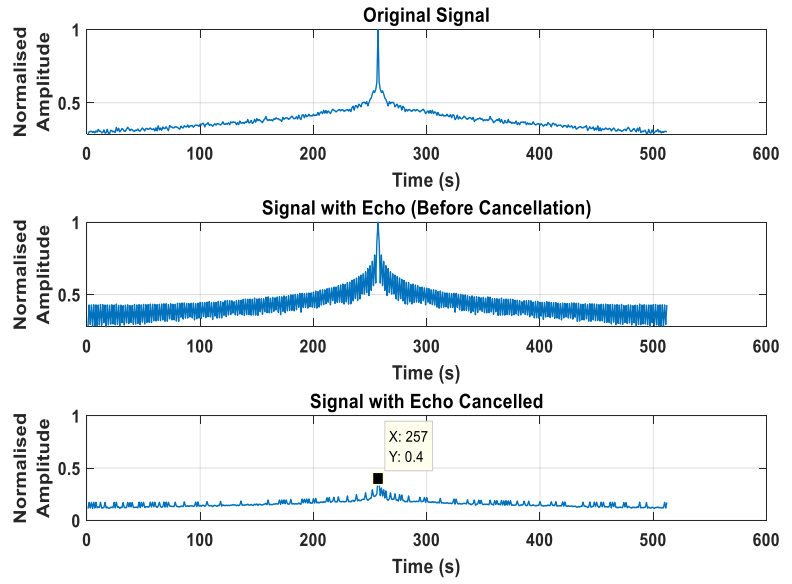
Images from dataset

Results

(a)

(b)

Figure 5. Resultant image of the IHGSOA-echo cancellation in SAR. (a) for SAR image 1 from dataset (b) for SAR image 2 from dataset
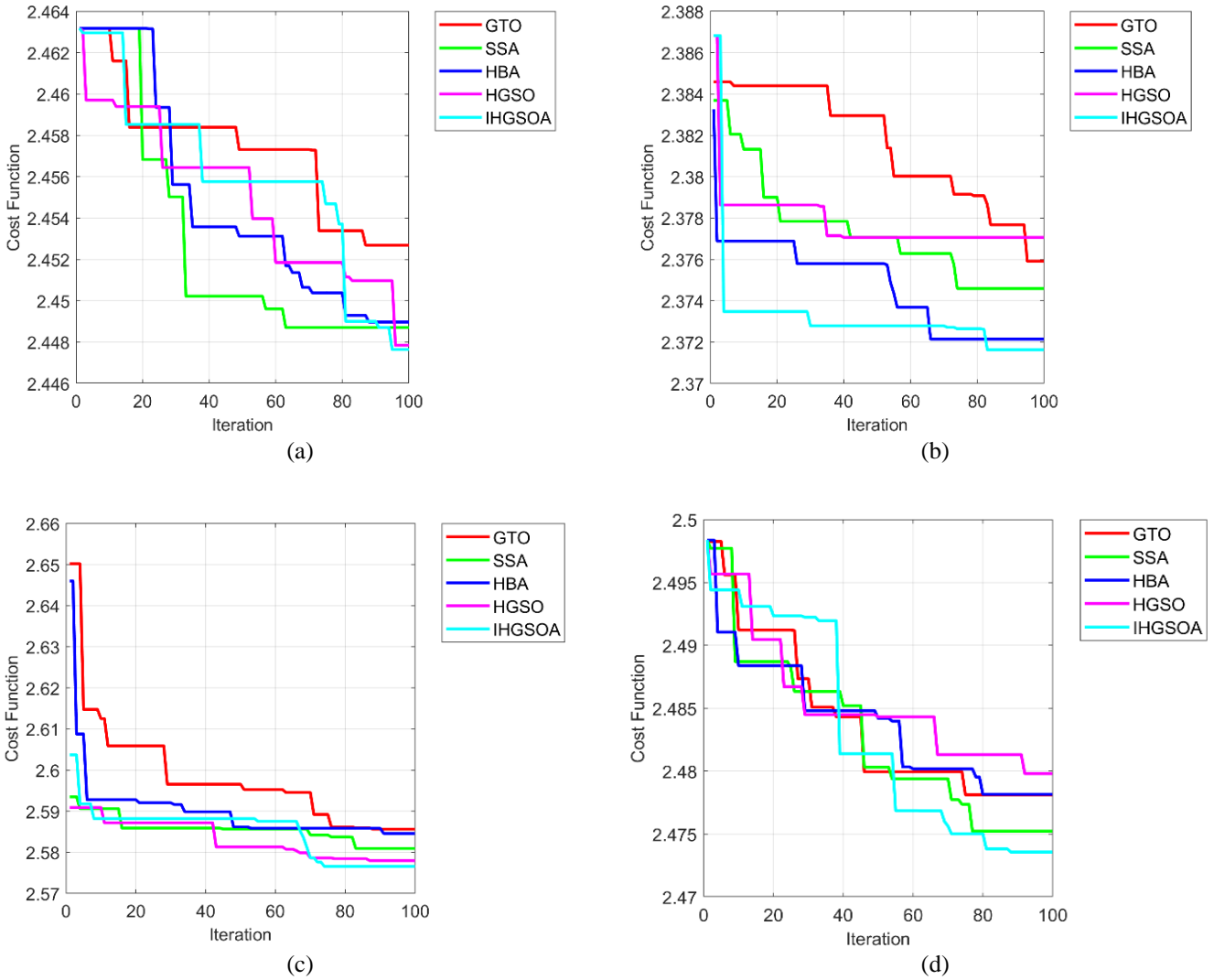

(a)

(b)

(c)

(d)

Figure 6. Convergence study of the heuristic-based echo cancellation in SAR for (a) SAR image 1; (b) SAR image 2; (c) SAR image 3; (d) SAR images 4 among conventional algorithms

6.4 Error assessment

The error assessment of the IHGSOA-based echo cancellation model is expressed in Figure 7. At mismatch degree 0.2, the error rate of the IHGSOA-based echo cancellation model is 14.28%, 12.85%, 8.57% and 2.85% for the SAR image 1. According to Figure 7(b), the error rate of the developed IHGSOA-based echo cancellation method is diminished with 9.72%, 4.16%, 2.77% and 1.38% for GTO, SSA, HBA and HGSO at the mismatch degree 0.5. From Figure 7(c), at the mismatch degree 0.9, the developed IHGSOA-based echo cancellation method gives a lower error rate for GTO, SSA, HBA and HGSO with 11.76%, 11.7%, 17.64% and 2.94%. Similarly, for Figure 7(d), the error rate of the IHGSOA-based echo cancellation model is diminished than GTO, SSA, HBA, and HGSO with 7.69%, 5.76%, 3.84% and 1.92% at the mismatch degree 0.3. According to these graphical results, the mistake occurrence of the IHGSOA-based echo cancellation method is minimized than the existing algorithms.
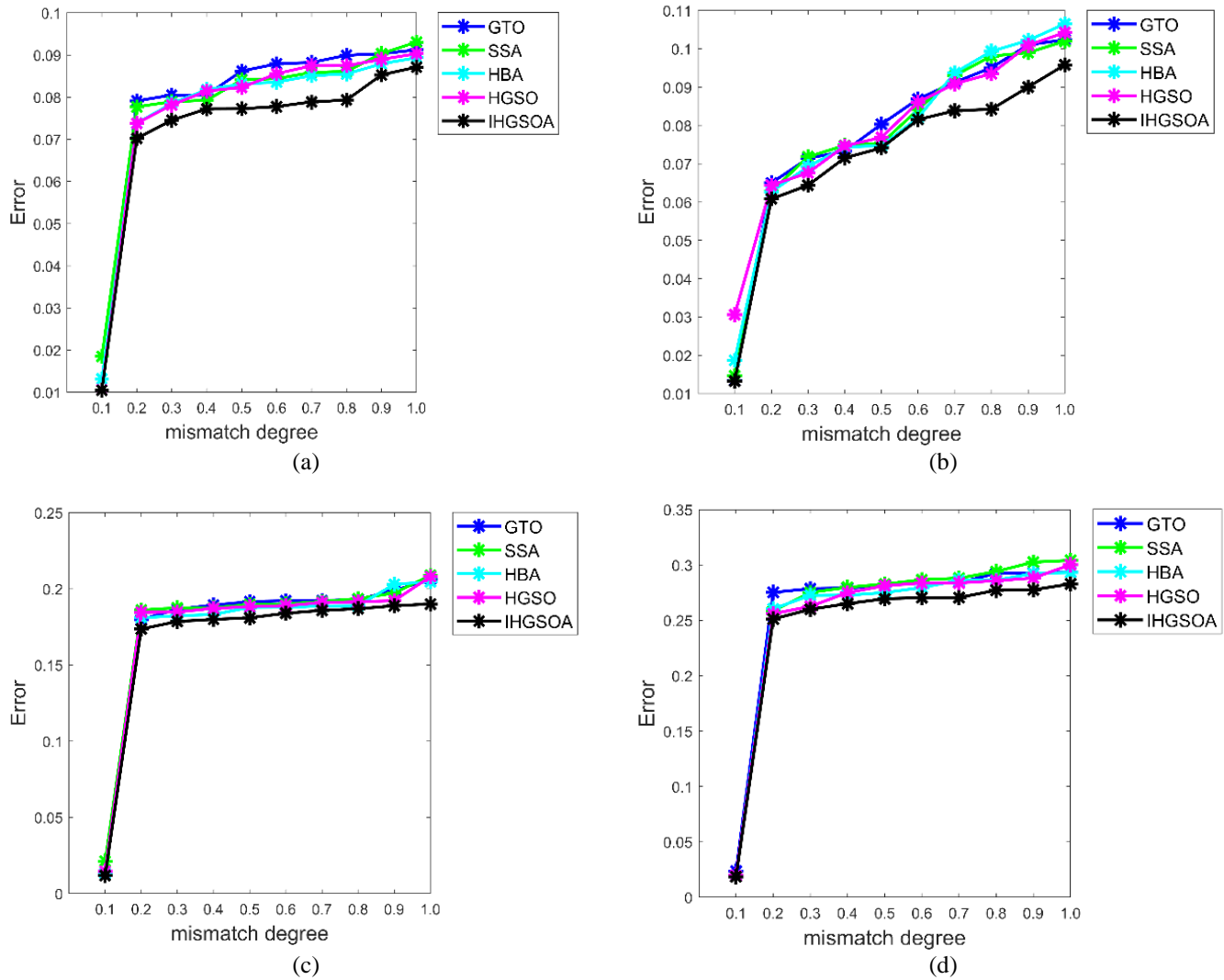

Figure 7. Error assessment of the heuristic-based Echo cancellation in SAR for (a) SAR image 1; (b) SAR image 2; (c) SAR image 3; (d) SAR image 4 across several existing algorithms

6.5 PAR investigation

The PAR investigation of the IHGSOA-based echo cancellation model in the SAR is illustrated in Figure 8. For the SAR image 4, the offered IHGSOA-based echo cancellation model has very low SAR with 0.37%, 0.83%, 0.04% and 0.12% for GTO, SSA, HBA and HGSO at mismatch degree 0.1. For the 3rd SAR image, the developed IHGSOA-based echo cancellation model attained lower PAR for GTO, SSA, HBA and HGSO with 0.32%, 0.40%, 0.16% and 0.36% at the mismatch degree taken as 0.5. According to the 2nd SAR image, the PAR of the developed IHGSOA-based echo cancellation model curtailed than the GTO, SSA, HBA and HGSO with 0.08%, 0.12%, 0.43% and 0.606% at the mismatch degree 0.3. Finally, for the 1st SAR image, the PAR value is decreased with GTO, SSA, HBA, and HGSO with 0.46%, 0.38%, 0.50% and 0.19% at the mismatch degree is taken as 0.6. Based on these line graphs, the PAR of the developed IHGSOA-based echo cancellation model is significantly lower than the usual algorithms.

The peak-average ratio, or PAR, as shown in Figure 8 for amplitude mismatch degrees ranging from 0.1 to 1. When amplitude mismatch is present, cancellation performance is quantitatively measured by PAR. It is clear that in the case of amplitude mismatch, a smaller PAR indicates that the object is more hidden in the SAR image. Figure 8 illustrates how PAR rises as the degree of mismatch increases. It shows that when there is an amplitude mismatch, cancelation

performance decreases.

Table 1 compares the PAR of the proposed IHGSOA algorithm with four existing methods (GTO, SSA, HBA, and HGSO) for four SAR images. IHGSOA consistently achieves the lowest PAR across all images, indicating better cancellation performance. For SAR image 1, IHGSOA's PAR is 2.6213, compared to higher values from other methods. Similarly, for SAR images 2, 3, and 4, IHGSOA outperforms with PAR values of 2.4156, 2.4732, and 2.5123, respectively.
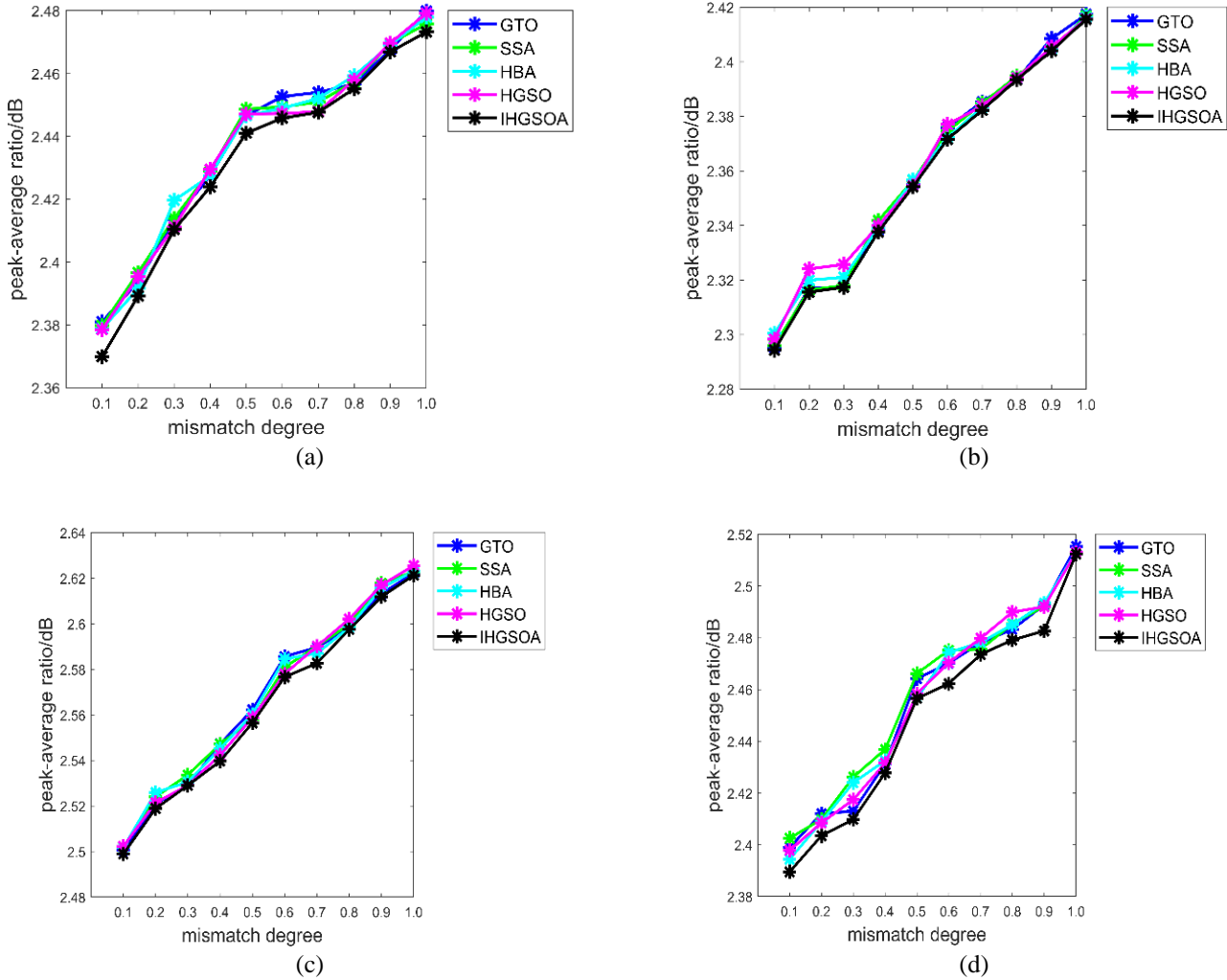

Figure 8. PAR assessment of the heuristic-based Echo cancellation in SAR for (a) SAR image 1; (b) SAR image 2; (c) SAR image 3; (d) SAR images 4

Table 1. Comparison of proposed IHGSOA with existing algorithms for PAR assessment for different SAR images

SAR Images	GTO	SSA	HBA	HGSO	IHGSOA	Inference
	PAR					
SAR image 1	2.6239	2.6225	2.6229	2.6234	2.6213	The IHGSOA achieves a lower PAR value compared to conventional algorithms across all SAR images.
SAR image 2	2.4165	2.4171	2.4166	2.4156	2.4156	
SAR image 3	2.4795	2.4779	2.4769	2.4762	2.4732	
SAR image 4	2.5142	2.5142	2.5131	2.5127	2.5123	

6.6 Comparison over the echo cancellation techniques

Figure 9 provides a detailed comparison of the proposed IHGSOA-based echo cancellation model with existing techniques, including ISRJ, LFM, GMTD, and NPISM. The comparison is made at a mismatch degree of 0.5. For the 1st SAR image, the IHGSOA model achieves a significantly lower error rate of 0.02%, outperforming the other methods with error rates of 0.03% for ISRJ and NPISM, 0.27% for LFM, and 0.31% for GMTD. This substantial reduction in error demonstrates the superior capability of the IHGSOA

model in accurately suppressing target echoes. Furthermore, the results confirm that the IHGSOA model consistently maintains a lower error and PAR across varying conditions, showcasing its robust performance and enhanced reliability compared to conventional echo cancellation techniques. This makes the IHGSOA model a more effective solution for improving target suppression in SAR images.

6.7 Statistical study of various algorithms

The statistical study of the IHGSOA-based echo

cancellation model is given in Table 2. At the 2nd SAR image, the standard deviation of the IHGSOA-based echo cancellation model is more progressed than the GTO, SSA, HBA and HGSO with 18.58%, 20.6%, 7.14% and 42.85%. Similarly, for SAR image 1, the standard deviation of the IHGSOA-based echo cancellation model is superior with 28.57%, 20%, 4.76% and 42.85%. For the 3rd SAR image, the developed IHGSOA-based echo cancellation model establishes higher standard deviation than the GTO, SSA, HBA and HGSO with 33.33%, 43.3%, 45.5% and 3.33%. For the final SAR image, the developed IHGSOA-based echo cancellation model has boosted standard deviation than the GTO, SSA, HBA and HGSO with 33.33%, 21.21%, 66.66% and 63.26%. Based on this graphical representation, the standard deviation of the IHGSOA-based echo cancellation method is raised than the existing algorithms.
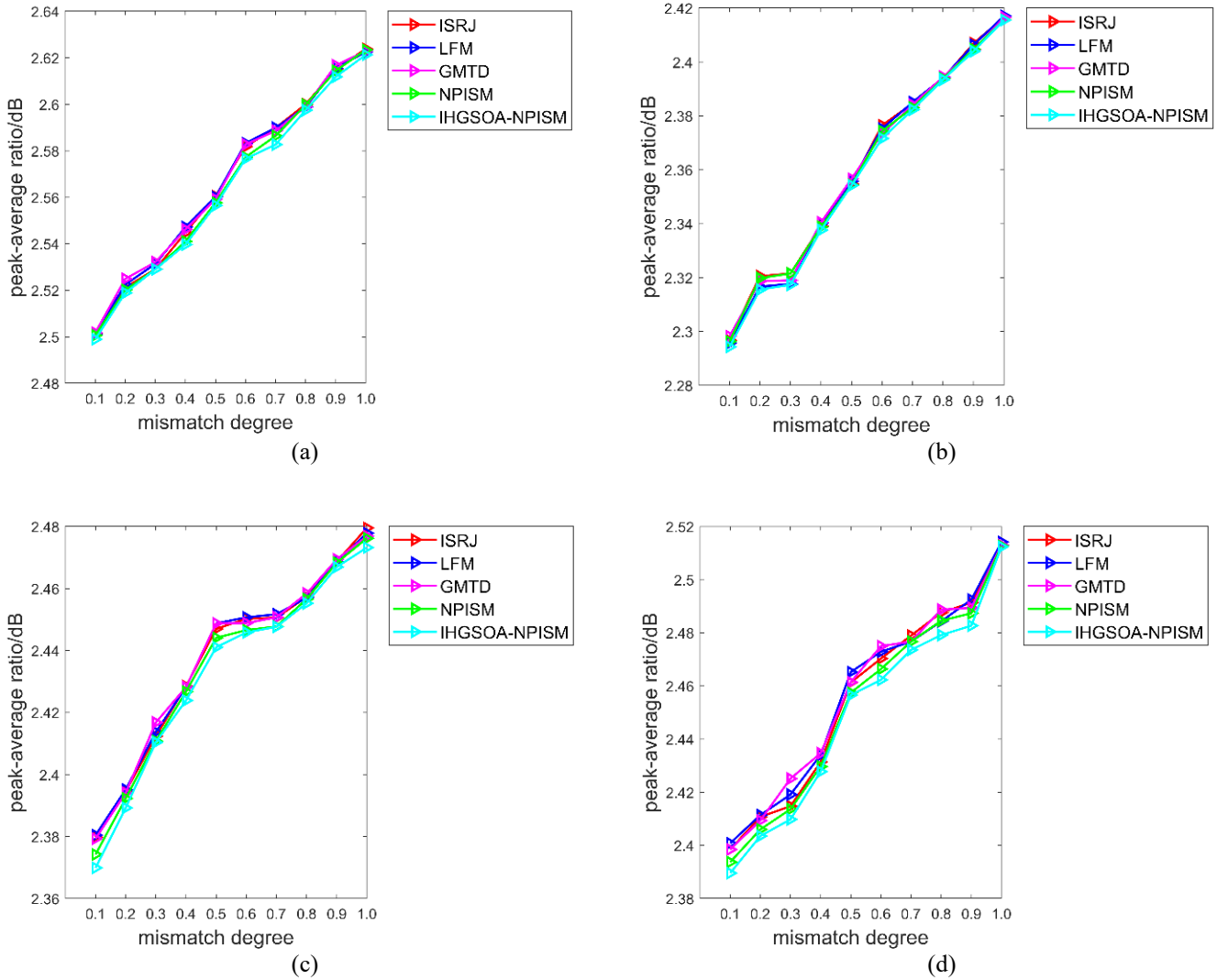
PAR

Figure 9. PAR assessment of the heuristic-based echo cancellation in SAR for (a) SAR image 1, (b) SAR image 2, (c) SAR image 3, (d) SAR images 4

Table 2. Statistical study of the developed heuristic-based echo cancellation model among various algorithms

Terms	GTO [28]	SSA [27]	HBA [29]	HGSO [26]	IHGSOA
SAR image 1					
Best	2.3759	2.3746	2.3721	2.3771	2.3716
Worst	2.3846	2.3837	2.3833	2.3868	2.3868
Mean	2.3815	2.3773	2.3746	2.3778	2.3732
Median	2.383	2.3771	2.3758	2.3771	2.3728
Standard deviation	0.002823	0.002524	0.002154	0.001491	0.00249
SAR image 2					
Best	2.3759	2.3746	2.3721	2.3771	2.3716
Worst	2.3846	2.3837	2.3833	2.3868	2.3868
Mean	2.3815	2.3773	2.3746	2.3778	2.3732
Median	2.383	2.3771	2.3758	2.3771	2.3728
Standard deviation	0.002823	0.002524	0.002154	0.001491	0.00249

6.8 Time-delay synchronization

An unavoidable processing time delay results in a time delay τ_d, which is incorporated into the intercepted received baseband signal as described in Eq. (11) and shown in Eq. (9). By adding this time delay, the cancellation signal and the original echo signal will match, resulting in effective echo cancellation. If there is a mismatch between the original echo signal and the cancellation signal, an error occurs at the output, leaving the target visible in the SAR image.

Figure 10 shows the Errors between the cancellation and echo signals for the proposed IHGSOA-based echo cancellation compared to existing techniques, with mismatch values ranging from 0.1 to 1. Across this range, the IHGSOA-based model consistently achieves lower error than conventional techniques.
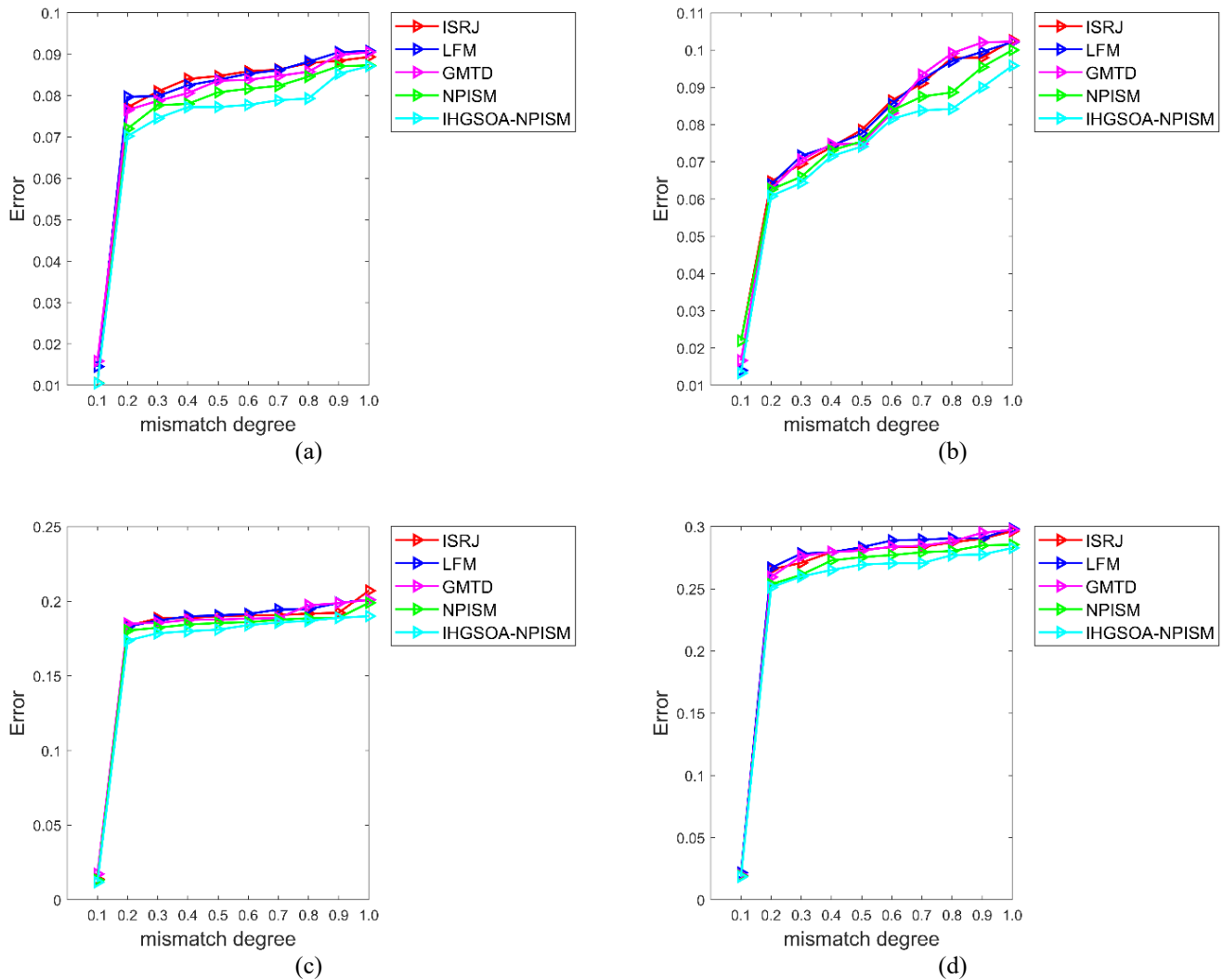
Errors

Figure 10. Error assessment of the heuristic-based echo cancellation in SAR for (a) SAR image 1; (b) SAR image 2; (c) SAR image 3; (d) SAR images 4

7. CONCLUSION

The IHGSOA-based optimal NP-ISM process is carried out to cancel the target echo in the SAR. After implementing the proposed method, the amplitude of cancellation signal matches with target echo at SAR receiver. Thus, the original echo present in the SAR will gets canceled. The simulation results show that the using the above cancelling system the amplitude of the target echo to reach SAR is reduced to 0.5 and 0.4 after cancellation. It is obvious that when applying proposed method, the desired target echo amplitude drops to 50% and 40% of its original target echo, hence the system has a very high cancellation effect thereby decreasing target visibility in SAR images. PAR increases with higher amplitude mismatch, indicating decreased cancellation performance and reduced object concealment in SAR images. The proposed IHGSOA-based echo cancellation model effectively aligns the cancellation and echo signals through time-delay synchronization, minimizing errors even in the presence of mismatch. It consistently outperforms conventional techniques, achieving lower errors across varying mismatch values. Also, demonstrates superior performance over conventional techniques by achieving consistently lower error rates and PAR values. Its robustness and reliability make it an effective solution for enhancing target concealment in SAR images, even under challenging mismatch conditions. The system can cancel the target echo effectively. the cost function of the IHGSOA-based echo

cancellation model is better than the GTO, SSA, HBA, and HGSO with 0.25%, 0.16%, 0.08% and 0.28% at iteration 100. The developed IHGSOA-based echo cancellation model has boosted standard deviation than the GTO, SSA, HBA and HGSO with 33.33%, 21.21%, 66.66% and 63.26%. Thus, the effectiveness of the newly developed approach is examined with the traditional echo cancellation system to determine the overall capability of the recommended echo cancellation model.

REFERENCES

[1] Wu, Q., Liu, J., Wang, J., Zhao, F., Xiao, S. (2018). Improved active echo cancellation against synthetic aperture radar based on nonperiodic interrupted sampling modulation. IEEE Sensors Journal, 18(11): 4453-4461. https://doi.org/10.1109/JSEN.2018.2824351

[2] Xu, L., Feng, D., Liu, Y., Pan, X., Wang, X. (2015). A three-stage active cancellation method against synthetic aperture radar. IEEE Sensors Journal, 15(11): 6173-6178. https://doi.org/10.1109/JSEN.2015.2453396

[3] Hanbali, S.B.S. (2019). Technique to counter improved active echo cancellation based on ISRJ with frequency shifting. IEEE Sensors Journal, 19(20): 9194-9199. https://doi.org/10.1109/JSEN.2019.2925004

[4] Anoosha, C., Krishna, B.T. (2020). Comparison on radar echo cancellation techniques for SAR jamming. In Microelectronics, Electromagnetics and Telecommunications: Proceedings of the Fifth ICMEET 2019, pp. 651-658. https://doi.org/10.1007/978-981-15-3828-5_67

[5] Yi, M., Huang, J., Ma, Y. (2017). An efficient echo cancelling scheme based on Nth-order SSC algorithm for nonlinear frequency modulated signal. Optik, 149: 229-238. https://doi.org/10.1016/j.ijleo.2017.09.014

[6] Wu, Q., Zhao, F., Wang, J., Liu, X., Xiao, S. (2019). Improved ISRJ-based radar target echo cancellation using frequency shifting modulation. Electronics, 8(1): 46. https://doi.org/10.3390/electronics8010046

[7] Nongpiur, R.C., Shpak, D.J. (2012). Maximizing the signal-to-alias ratio in non-uniform filter banks for acoustic echo cancellation. IEEE Transactions on Circuits and Systems I: Regular Papers, 59(10): 2315-2325. https://doi.org/10.1109/TCSI.2012.2185333

[8] Liu, Z., Li, Z., Yu, H., Wu, J., Huang, Y., Yang, J. (2018). Bistatic forward-looking SAR moving target detection method based on joint clutter cancellation in echo-image domain with three receiving channels. Sensors, 18(11): 3835. https://doi.org/10.3390/s18113835

[9] Zhou, Q., Zhou, S., Yang, L., Ning, X., Xing, M. (2021). Synthetic aperture radar interference based on scene fusion and active cancellation. IEEE Journal of Selected Topics in Applied Earth Observations and Remote Sensing, 14: 10375-10382. https://doi.org/10.1109/JSTARS.2021.3117849

[10] Cheng, S., Sun, X., Cai, Y., Zheng, H., Yu, W., Zhang, Y., Chang, S. (2022). A joint azimuth multichannel cancellation (JAMC) antibarrage jamming scheme for spaceborne SAR. IEEE Journal of Selected Topics in Applied Earth Observations and Remote Sensing, 15: 9913-9926. https://doi.org/10.1109/JSTARS.2022.3221402

[11] Lv, X., Xing, M., Deng, Y., Zhang, S., Wu, Y. (2009).

Coherence-improving algorithm for image pairs of bistatic SARs with nonparallel trajectories. IEEE Transactions on Geoscience and Remote Sensing, 47(8): 2884-2898. https://doi.org/10.1109/TGRS.2009.2018532

[12] Shi, S., Li, C., Hu, J., Zhang, X., Fang, G. (2021). A high frequency vibration compensation approach for terahertz SAR based on sinusoidal frequency modulation Fourier transform. IEEE Sensors Journal, 21(9): 10796-10803. https://doi.org/10.1109/JSEN.2021.3056519

[13] Zhu, H., Yu, Z., Yu, J. (2022). Sea clutter suppression based on complex-valued neural networks optimized by PSD. IEEE Journal of Selected Topics in Applied Earth Observations and Remote Sensing, 15: 9821-9828. https://doi.org/10.1109/JSTARS.2022.3218055

[14] Mahbub, U., Fattah, S.A. (2014). Gradient based adaptive algorithm for echo cancellation from recorded echo corrupted speech. Advances in Electrical Engineering, 2014(1): 869721. https://doi.org/10.1155/2014/869721

[15] Thepie Fapi, E.R., Pastor, D., Beaugeant, C., Taddei, H. (2010). Acoustic echo cancellation embedded in smart transcoding algorithm between 3GPP AMR-NB modes. Journal of Electrical and Computer Engineering, 2010(1): 902569. https://doi.org/10.1155/2010/902569

[16] Chan, Y.K., Chua, M.Y., Koo, V. (2009). Sidelobes reduction using simple two and tri-stages non linear frequency modulation (NLFM). Progress In Electromagnetics Research, 98: 33-52. https://doi.org/10.2528/PIER09073004

[17] Guan, X., Hu, D.H., Zhong, L.H., Ding, C.B. (2014). Strong echo cancellation based on adaptive block notch filter in passive radar. IEEE Geoscience and Remote Sensing Letters, 12(2): 339-343. https://doi.org/10.1109/LGRS.2014.2339826

[18] Meller, M. (2012). Cheap cancellation of strong echoes for digital passive and noise radars. IEEE Transactions on Signal Processing, 60(5): 2654-2659. https://doi.org/10.1109/TSP.2012.2187286

[19] Hanbali, S.B.S. (2019). Technique to counter improved active echo cancellation based on ISRJ with frequency shifting. IEEE Sensors Journal, 19(20): 9194-9199. https://doi.org/10.1109/JSEN.2019.2925004

[20] Zhao, D., Wang, J., Chen, G., Wang, J., Guo, S. (2020). Clutter cancellation based on frequency domain analysis in passive bistatic radar. IEEE Access, 8: 43956-43964. https://doi.org/10.1109/ACCESS.2020.2977961

[21] Tang, M.C., Wang, F.K., Horng, T.S. (2017). Single self-injection-locked radar with two antennas for monitoring vital signs with large body movement cancellation. IEEE Transactions on Microwave Theory and Techniques, 65(12): 5324-5333. https://doi.org/10.1109/TMTT.2017.2768363

[22] Trizna, D.B. (1997). A model for Brewster angle damping and multipath effects on the microwave radar sea echo at low grazing angles. IEEE Transactions on Geoscience and Remote Sensing, 35(5): 1232-1244. https://doi.org/10.1109/36.628790

[23] Cooper, K.B., Durden, S.L., Roy, R.J., Siles, J.V., Monje, R.R., Dengler, R., Beauchamp, R. (2021). Improving FM radar dynamic range using target phase noise cancellation. IEEE Journal of Microwaves, 1(2): 586-592. https://doi.org/10.1109/JMW.2021.3061887

[24] Shi, T., Liang, D., Han, M., Chen, Y. (2022). Photonics-

based de-chirping and leakage cancellation for frequency-modulated continuous-wave radar system. IEEE Transactions on Microwave Theory and Techniques, 70(9): 4252-4262. https://doi.org/10.1109/TMTT.2022.3186375

[25] Hashim, F.A., Houssein, E.H., Mabrouk, M.S., Al-Atabany, W., Mirjalili, S. (2019). Henry gas solubility optimization: A novel physics-based algorithm. Future Generation Computer Systems, 101: 646-667. https://doi.org/10.1016/j.future.2019.07.015

[26] Mirjalili, S., Gandomi, A.H., Mirjalili, S.Z., Saremi, S., Faris, H., Mirjalili, S.M. (2017). Salp Swarm Algorithm: A bio-inspired optimizer for engineering design problems. Advances in Engineering Software, 114: 163-191. https://doi.org/10.1016/j.advengsoft.2017.07.002

[27] Kareem, S.S., Mostafa, R.R., Hashim, F.A., El-Bakry, H.M. (2022). An effective feature selection model using hybrid metaheuristic algorithms for IoT intrusion detection. Sensors, 22(4): 1396. https://doi.org/10.3390/s22041396

[28] Hashim, F.A., Houssein, E.H., Hussain, K., Mabrouk, M.S., Al-Atabany, W. (2022). Honey Badger Algorithm: New metaheuristic algorithm for solving optimization problems. Mathematics and Computers in Simulation, 192: 84-110. https://doi.org/10.1016/j.matcom.2021.08.013